Inelastic neutron scattering study of ordered gamma -ZrH

1994 J. Phys.: Condens. Matter 6 8989

(http://iopscience.iop.org/0953-8984/6/43/005)

J. Phys.: Condens. Matter 6 (1994) 8989–9000. Printed in the UK

Inelastic neutron scattering study of ordered γ-ZrH

A I Kolesnikov†‡, I O Bashkin†, A V Belushkin§‖, E G Ponyatovsky† and M Prager‡

† Institute of Solid State Physics of the Russian Academy of Sciences, 142432 Chernogolovka, Moscow District, Russia

‡ Institut für Festkörperforschung, Forschungszentrum Jülich KFA, D-52425 Jülich, Germany

§ Frank Laboratory of Neutron Physics, Joint Institute for Nuclear Research, 141980, Dubna, Moscow District, Russia

‖ Rutherford Appleton Laboratory, Chilton, Didcot, Oxon OX11 0QX, UK

Received 7 July 1994

Abstract. Lattice dynamics of the ordered γ-ZrH phase was studied by inelastic neutron scattering (INS). It was found that the hydrogen optical peak in the INS spectrum had three maxima at energy transfers of 141.5, 148.7 and 156.3 meV. The peak was accurately described using the Born–von Kármán model. Anharmonicity of hydrogen vibrations was evident in the high-energy range of the spectrum from a strong sharp peak at $E = 269.7$ meV and broader features below the bands of free-multiphonon scattering. These anharmonic phenomena were attributed to the bound multiphonon states (biphonon, triphonon, tetraphonon and their combinations), and the values of the binding energies of biphonons and triphonons were obtained from the experimental data.

1. Introduction

The structure and lattice dynamics of γ-ZrD have been studied recently using neutron diffraction and inelastic neutron scattering (INS) [1]. It was found that γ-ZrD had approximately stoichiometric composition and had a face-centred orthorhombic metal sublattice with axial ratios $b/a \simeq 1.015$ and $c/a \simeq 1.091$. Deuterium atoms occupied the tetrahedral interstices on alternate {110} planes, and the space group was $Cccm$ rather than $P4_2/n$ assumed earlier [2]. Thus, the γ-ZrD structure proved to be similar to that of γ-TiH(D) [3–5].

The γ phase in the Ti–H and Zr–H systems is unique among the hydride phases. The H–H distance along the crystal c-axis is shorter than those in the ab plane by a factor of $\sqrt{2}/1.09 \simeq 1.3$. Therefore, this phase can be considered as a hydride where the H–H interaction is essentially one dimensional.

Previous INS experiments have shown that H(D) vibrations in γ-TiH, γ-TiD [6–8] and γ-ZrD [1] were highly anharmonic. Each spectrum had a peak below the band of free two-phonon scattering, and somewhat broader features were observed below the higher-harmonic multiphonon bands. These anharmonic effects have been discussed in terms of bound multiphonon states, i.e. biphonon, triphonon and tetraphonon excitations, which were proposed for a lattice dynamic description of systems with large anharmonicity (for a review see [9]).

In this work we measured the INS spectrum of $(\alpha + \gamma)$-$ZrH_{0.68}$ which contains just one hydride phase, γ, the rest being α-Zr. The anticipated splitting of the hydrogen optical peak

0953-8984/94/438989+12$19.50

as well as the anharmonic features at the multiphonon bands are found. Their nature and the isotope effects are discussed.

2. Experimental

To prepare the sample, a Zr ingot of 99.96 at.% purity was heated in a vacuum of $\sim 7 \times 10^{-3}$ Pa to 1070 K and allowed to absorb gaseous hydrogen which was obtained by thermal decomposition of TiH_2. The hydrogen content was determined from the weight gain, $x = H/Zr = 0.68 \pm 0.01$. The hydrogenated sample was aged at ambient temperature for nine years. Six plates of $23 \times 45 \times 0.6\,mm^3$ size were then spark-cut from the $ZrH_{0.68}$ ingot, mechanically polished and etched in $HF+HNO_3$. An x-ray test demonstrated that the $ZrH_{0.68}$ sample thus prepared consisted of two phases, γ and α. The α phase (space group $P6_3/mmc$) has a HCP lattice with a hydrogen content close to zero at helium temperature [2].

INS measurements were carried out at 4.5 K using the time-focused crystal analyser (TFXA) spectrometer [10] at the spallation neutron source, ISIS, Rutherford Appleton Laboratory, UK. The spectrometer provided an excellent resolution, $\Delta\omega/\omega \leqslant 2\%$, in the range of energy transfer 2–500 meV. The data were transformed to $S(Q, \omega)$ against energy transfer (meV) using standard programs. The background from the empty can in the cryostat was measured under the same conditions and subtracted from the experimental data.

To control the phase content of the sample, neutron diffraction was measured at the TFXA spectrometer simultaneously with INS. It also confirmed that the sample consisted of two phases only, γ-ZrH and α-Zr.

3. The INS spectrum

The experimental INS spectrum $S(Q, \omega)$ for the $(\alpha+\gamma)$-$ZrH_{0.68}$ sample is shown in figure 1 (points). Excitations are observed at various different energy transfers: (i) the lower range, 0–30 meV, is usually associated with vibrations of heavy metal atoms in the hydrides; (ii) the medium range, 135–160 meV, is due to hydrogen optical modes in γ-ZrH; and (iii) the range above 250 meV is related to multiphonon processes of neutron scattering on the hydrogen atoms.

3.1. Multiphonon contributions to the one-phonon spectrum

The contribution from multiphonon neutron scattering was calculated in the harmonic isotropic approximation up to four-phonon processes by an iterative technique using multiconvolution of the one-phonon spectrum [6, 11]. Experimental data in the energy range of the lattice and hydrogen optic phonons, 2–160 meV, were accepted at the first iterative step as the one-phonon spectrum of hydrogen vibrations. To take into account only the contribution from hydrogen atoms, the intensity of the spectrum in the range of lattice vibrations was multiplied by a factor of 0.60. This factor appeared for the following reason. Calculation of the γ-ZrH lattice dynamics in section 3.2 showed that the ratio of integrated partial intensities $S(Q, \omega)$ for zirconium and hydrogen atoms is equal to 0.45 in the range of lattice vibrations. The same efficiency was assumed for the contribution of Zr atoms in the α phase. The above factor 0.60 was then obtained from the phase content in the sample, 32% α and 68% γ.

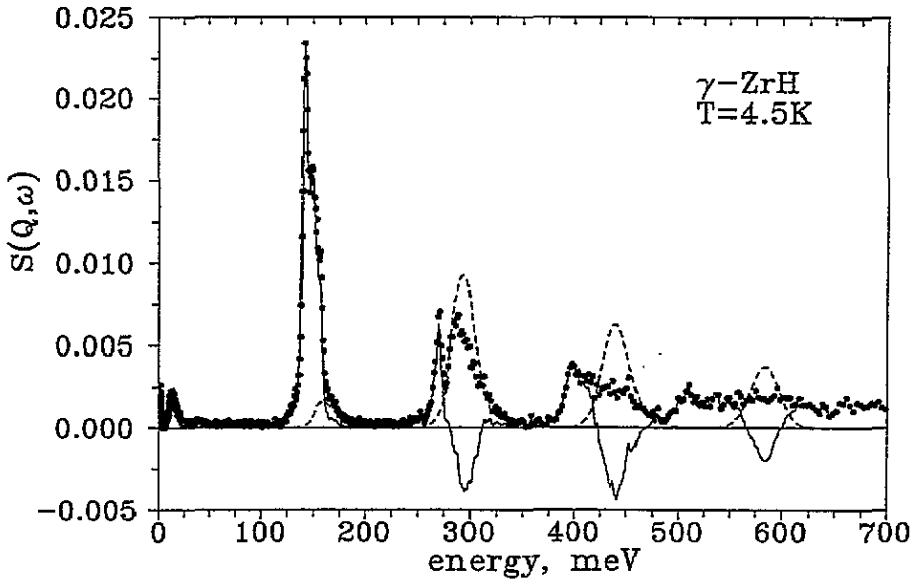

Figure 1. The INS spectrum $S(Q, \omega)$ of the $(\alpha + \gamma)$-$ZrH_{0.68}$ at 4.5 K (points). The calculated multiphonon contribution is shown as a broken curve; the full curve represents the difference between the experimental data and the calculated multiphonon spectrum.

At the next iterative step the calculated multiphonon contributions were subtracted from the initial experimental spectrum, and the result was accepted as a new one-phonon spectrum (in the energy range 2–160 meV). Convergence was achieved in three iterations.

The results of the calculation are shown in figure 1, where the contributions from the multiphonon neutron scattering are plotted as a broken curve and the difference between the experimental and multiphonon spectra is drawn as a full curve.

3.2. Hydrogen optic modes

For the sake of quantitative comparison, the fundamental hydrogen peak in the γ-ZrH spectrum was treated as a sum of three Gaussians (short-dash broken curve in figure 2). The parameters of the fitted Gaussians are listed in table 1. The table also includes similar data for the γ-ZrD spectrum measured at TFXA [1]. It follows from the data that ratios $\omega_i^{\mathrm{H}}/\omega_i^{\mathrm{D}}$ for all three components of the peaks are smaller than $\sqrt{m_{\mathrm{D}}/m_{\mathrm{H}}} = \sqrt{2}$, as should be the case for a harmonic oscillator. This deviation from the square-root mass ratio is indicative of anharmonicity of H(D) vibrations in γ-ZrH(D), and it is of nearly the same magnitude as for titanium monohydride, γ-TiH(D) [6–8].

Many INS experiments were performed with the other phases of the Zr–H system. A very broad peak due to hydrogen vibrations has been observed on HCP α-ZrH_y, $y = 0.03$–0.05, at an energy of 143–144 meV [12, 13]. The FCC δ phase in ZrH_y, $0.54 \leqslant y \leqslant 1.56$, showed a broad peak at 130–140 meV [14–20]. The FCT ε-ZrH_y, $1.9 \leqslant y \leqslant 2$, had a split peak with maxima at energies 136–138 meV and 143–145 meV and with a high-energy shoulder at 154 meV [19–21]. The shoulder was related to the multiphonon processes which combined optical and acoustic vibration [21]. Thus, the optical peak in the γ phase has the highest energy compared to the other phases of the Zr–H system. This is systematically related to the metal-to-hydrogen distances in zirconium hydrides. The distance in the γ phase

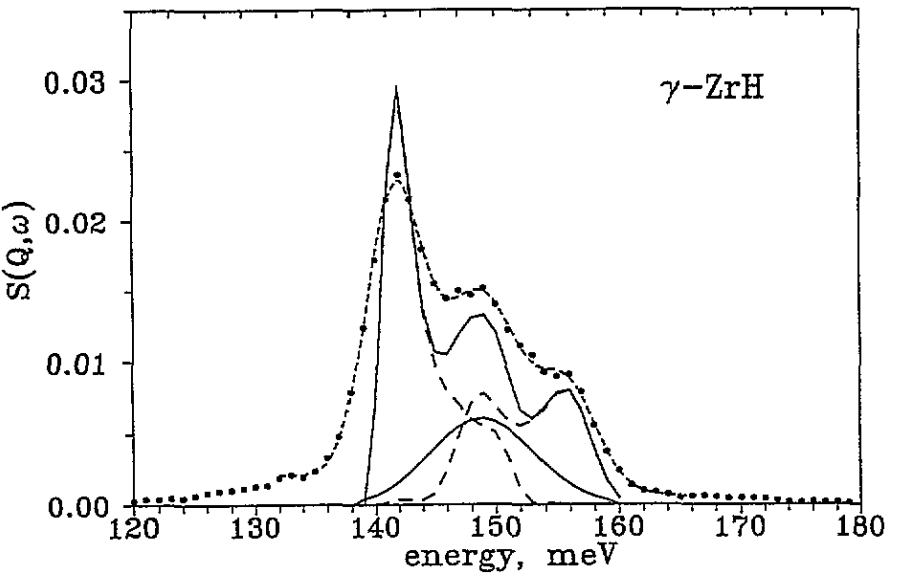

Figure 2. Experimental (points) and calculated (top full curve) $S(Q,\omega)$ spectra of the γ phase in the range of hydrogen optical modes (calculated multiphonon contributions are subtracted from the experimental data). The calculated spectrum was convoluted with the model resolution function of the TFXA spectrometer (a triangle with a width at half-maximum of $\Delta E = 0.02\omega$). The contributions to the calculated spectrum from vibrations of H atoms in the *ab* plane and along the *c* axis are shown as long-dash broken curves (left and split right peaks, respectively). The peak below (full curve) represents the states that form bound multiphonon states.

Table 1. Peak positions, ω_i (meV), full widths at half-maximum, δ_i (meV), and peak amplitudes, H_i (arbitrary units), of Gaussians that describe the H and D optical bands in the INS spectra of γ-ZrH (present data) and γ-ZrD [1]. The line $\omega_i^{\mathrm{H}}/\omega_i^{\mathrm{D}}$ shows deviation from the harmonic value $\sqrt{m^{\mathrm{D}}/m^{\mathrm{H}}} = \sqrt{2}$.

	γ-ZrH			γ-ZrD		
	$i=1$	$i=2$	$i=3$	$i=1$	$i=2$	$i=3$
ω_i	141.6	148.8	156.0	103.4	108.0	112.7
$\omega_i^{\mathrm{H}}/\omega_i^{\mathrm{D}}$	1.37	1.38	1.38			
δ_i	5.5	7.8	5.4	4.4	4.9	4.8
H_i	0.50	0.33	0.16	0.37	0.27	0.20

is $R_{\mathrm{Zr-D(H)}} = 2.041$ Å [1], but increases to 2.070 Å and 2.082 Å in the δ and ε phases, respectively [2].

Another dependence of the hydrogen optical frequency is observed for α and γ phases. The interatomic distance in the α phase, $R_{\mathrm{Zr-H(D)}} = 2.011$ Å at 873 K [2], is shorter than in γ-ZrH, but the energy of hydrogen vibrations is lower than in the γ phase.

The $\omega(R_{\mathrm{M-H}})$ dependence in other M–H systems is usually described by the $1/R^n$ law, where $1 \leqslant n \leqslant 2$ [22–26]. This law is also valid for the series of α-ZrH_y, δ-ZrH_y and ε-ZrH_y. The $\omega(R_{\mathrm{Zr-H}})$ behaviour becomes anomalous when γ-ZrH is included in the series. This indicates that the potential for hydrogen atoms in the γ-ZrH is steeper than in any other Zr–H phase.

The structure of the optical band in the γ-ZrH spectrum is very similar to that in γ-ZrD [1]. A good description of the γ-ZrD optical band was given within the Born–von Kármán model [1]. A similar calculation was carried out here for γ-ZrH on the basis of γ-ZrD interatomic force constants.

Each pairwise interaction was described with two parameters, i.e. the longitudinal (L) and transverse (T) force constants. Five kinds of pairs were involved in the calculation, i.e. the nearest Zr–Zr and Zr–D atoms and the first-, second- and third-nearest D–D neighbours. The interatomic distances for the D–D pairs were $c/2$ along the crystal c-axis, $\sqrt{a^2+b^2}/2$ in the ab plane and $\sqrt{a^2+b^2+c^2}/2$ in the (111) direction, respectively. The interatomic force constants used in this work are based on those obtained for γ-ZrD [1], but adapted to the Zr–H system. The Zr–H interaction determines the average energy of hydrogen vibrations. It was necessary, therefore, to take into account the observed anharmonicity of the H(D) vibrations. The energies of the main features in the peak of H(D) vibrations in the experimental spectra relate as $\omega_1^{\mathrm{H}}/\omega_1^{\mathrm{D}} \simeq 1.37$ (table 1) rather than $\sqrt{2}$ required for a harmonic crystal. Since force constants are proportional to ω^2, the Zr–H and Zr–D force constants should relate as $(1.37/\sqrt{2})^2 \simeq 0.94$. Therefore, the Zr–D force constants were reduced in the present calculation by a factor of 0.94. The total set of model constants is given in table 2.

Table 2. The longitudinal (L) and transverse (T) force constants (in $\mathrm{N\,m^{-1}}$) in the Born–von Kármán model calculations.

	First neighbour		Second neighbour		Third neighbour	
	L	T	L	T	L	T
H–H = D–D	3.0	1.5	−1.5	0.	1.0	0.
Zr–H = 0.94× (Zr–D)	29.5	14.8				
Zr–Zr	8.0	0.				

The UNISOFT program [27] was used for the calculations. The weighted densities of phonon states were obtained according to

$$G_i(\omega) = \frac{1}{3Nm_i} \sum_{j,q} |e(i|qj)|^2 \delta\big(\omega - \omega_j(q)\big) \tag{1}$$

where $\omega_j(q)$ and $e(i|qj)$ are eigenvalues and eigenvectors of the dynamical matrix corresponding to the phonon state qj, and m_i is the mass of atom i. The summation runs over $N = 1728$ points in the q-space distributed uniformly over the reduced Brillouin zone. To compare with the experimental spectrum, we transformed the calculated data to

$$S(Q,\omega) = (\hbar Q^2/6\omega) \sum_i \exp(-2\mathrm{DW}_i)\sigma_i G_i(\omega)[n(\omega)+1] \tag{2}$$

where Q is the neutron momentum transfer, DW_i is the Debye–Waller factor of atom i, σ_i is the neutron scattering cross section of atom i, and $n(\omega)$ is the Bose factor.

The calculated $S(Q,\omega)$ spectrum of γ-ZrH is represented by the top full curve in figure 2. It fits the experimental points with reasonable accuracy. The contribution to the calculated spectrum from H atoms which vibrate in the ab-plane (the left peak) and along the c-axis (the split peak at the right) are shown in figure 2 as long-dash broken curves.

The good correspondence between the calculated and experimental spectra for γ-ZrH as well as for γ-ZrD [1] proves that the force constants both of the H–H interaction and of the D–D interaction are actually the same, in spite of anharmonic behaviour of H(D) vibrations.

It is interesting to compare the optical phonon band of γ-ZrH with the impurity hydrogen vibrations in γ-ZrD (figure 3). A hydrogen impurity of about 0.9% was found in the previous study on γ-ZrD [1]. This impurity hydrogen resulted in a narrow split peak in the γ-ZrD INS spectrum (full points and the broken curve). It was assumed from the intensity distribution and the small width of the peak that the impurity hydrogen vibrations should be discussed in terms of local oscillators rather than optical phonon modes. Two maxima of the split hydrogen peak in the INS spectrum of γ-$ZrD_{0.991}H_{0.009}$ were observed at 147.2 and 154.3 meV [1]. The values of the first H and D optic peaks in the INS spectrum of γ-$ZrD_{0.991}H_{0.009}$ exactly follow the harmonic behaviour. The dispersive optic phonon band in γ-ZrH is very different from the impurity hydrogen peak (figure 3). The average energy of the impurity peak in γ-ZrD is higher than that of the γ-ZrH optic band. This is indicative of larger force constants for the Zr–H interaction in γ-ZrD than in γ-ZrH. Thus, it can be concluded that the pair potential for the Zr–H interaction in the γ phases is somewhat different for zirconium hydride and deuteride.

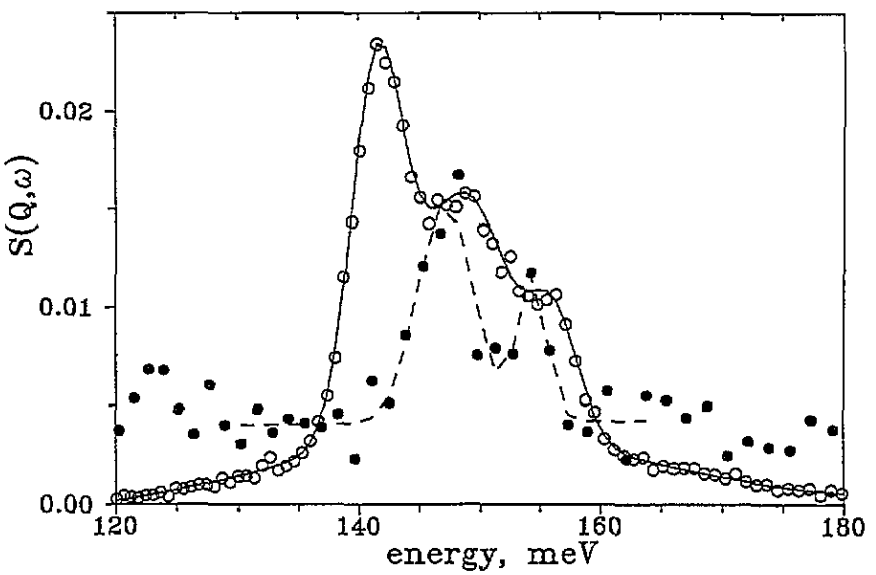

Figure 3. Experimental $S(Q,\omega)$ spectra of γ-ZrH (open points) and γ-$ZrD_{0.991}H_{0.009}$ (full points) [1] in the range of hydrogen optical modes.

3.3. Lattice vibrations

Figure 4 shows the generalized vibrational densities of states $\Theta(\omega)$ in the range 0–30 meV as obtained from the experimental (points) and calculated (full curve) $S(Q,\omega)$ spectra according to

$$\Theta(\omega) = \frac{\exp(2\mathrm{DW})S(Q,\omega)\omega}{Q^2[n(\omega)+1]}. \tag{3}$$

The density of phonon states of α-Zr at room temperature [28] is also presented in figure 4 (short-dash broken curve at the bottom). This density of states is normalized under the assumption that 32% of the content of our sample consist of the α phase, and Zr atoms in both α and γ phases show the same efficiency of neutron scattering. In spite of the rather crude fit of the Zr–Zr force constants for γ-ZrD [1], their use in the present calculations also gives a fairly good agreement with the experiment in the lattice part of the γ-ZrH spectrum.

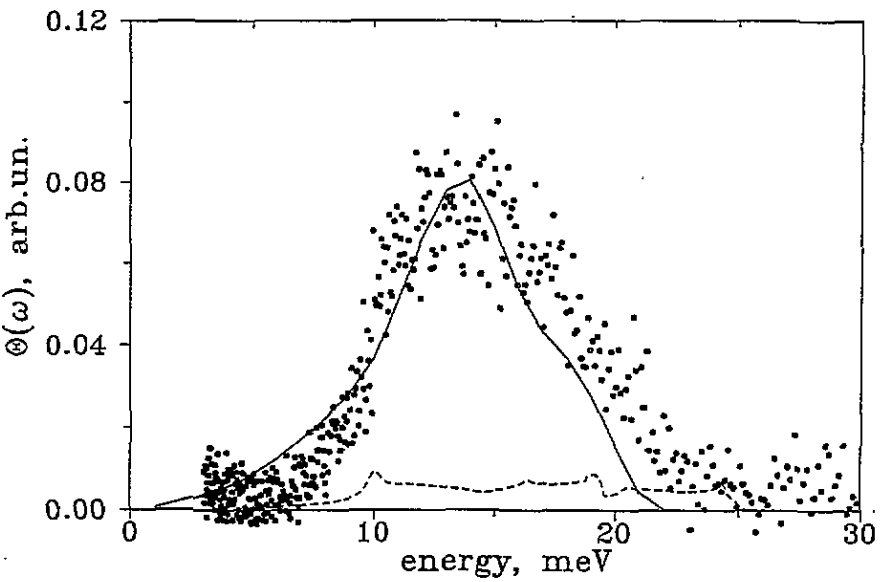

Figure 4. Generalized vibrational densities of states, $\Theta(\omega)$, of $(\alpha+\gamma)$-$ZrH_{0.68}$ in the range of lattice vibrations. Experimental points were calculated from the measured $S(Q,\omega)$ spectrum using (3). The calculated $\Theta(\omega)$ spectrum of γ-ZrH (present work) and the density of phonon states of α-Zr [28] are shown as full and broken curves, respectively.

The calculated generalized vibrational density of states of γ-ZrH in the range of lattice vibrations is compared to that of γ-ZrD in figure 5 (full curves), where both spectra are normalized to unity. There is an evident difference between the spectra. Partial $\Theta(\omega)$ spectra for zirconium atoms in both γ-ZrH and γ-ZrD are the same, and partial $\Theta(\omega)$ for H and D atoms are identical. But $\Theta(\omega)$ for Zr atoms essentially differs from that for H atoms.

Then different contributions from the partial $\Theta(\omega)$ for Zr (short-dash broken curves) and H or D (long-dash broken curves) atoms result in different total spectra. The contribution from Zr atoms dominates in the γ-ZrD spectrum because the weighted density of phonon states for Zr atoms is larger than for D (as well as for H) atoms. But the relation is opposite for γ-ZrH due to the large neutron scattering cross section of H atoms compared to those of Zr atoms.

The obtained ratio of the partial integrated intensities for the lattice part of the $\Theta(\omega)$ spectra for the H and Zr atoms was used for the multiphonon calculations in the section 3.1.

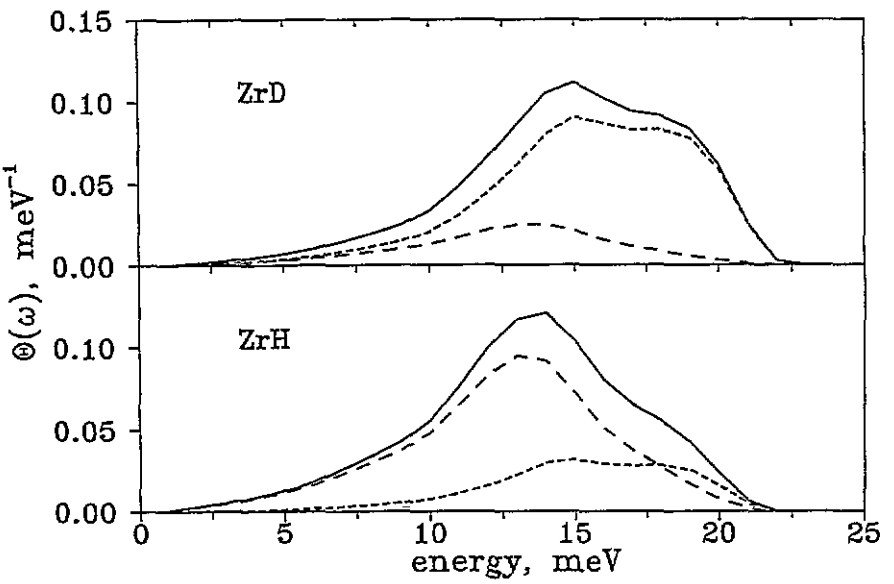

Figure 5. Calculated generalized vibrational densities of states $\Theta(\omega)$ (full curves) for γ phases of ZrH and ZrD in the range of lattice vibrations. The contributions to the spectra from the Zr and H(D) atoms are shown by short-dash and long-dash broken curves, respectively.

3.4. The range of multiphonon scattering

The calculated multiphonon spectrum in figure 1 describes only parts of the experimental data. There are some strong features that remain unattributed in the harmonic approximation. They are clearly seen in the difference curve between the experimental spectrum and the calculated multiphonon contributions (full curve in figure 1). They appear as a peak or a broader band at an energy below a harmonic band followed by a negative peak, i.e. the intensity deficit in the harmonic band of multiphonon scattering. This is further evidence of the essential anharmonicity of γ-ZrH.

The nature of equivalent such extra peaks in γ-TiH(D) and γ-ZrD has been treated in terms of the strong interaction between optical phonons [1, 6–8]. It has been shown theoretically [9, 29–31] that the strong phonon interaction can result in bound multiphonon states (biphonons and triphonons) which do not occur in a harmonic crystal. Such a quasi-particle is characterized by the appropriate energy and wavevector, similar to phonons. The

theory gives a simple relationship between the energies of biphonon and triphonon states and the anharmonicity parameters A and $\tilde{A}$ which determine the strength of the two- and three-phonon interaction [29–31]:

$$E_2 = 2\omega - 2A \qquad E_3 = 3\omega - 6(A + \tilde{A}) \tag{4}$$

where ω is the energy of optical phonons. There is some uncertainty in the value of the energy of the one-phonon mode, ω, because the experimental optic band is rather broad and structured.

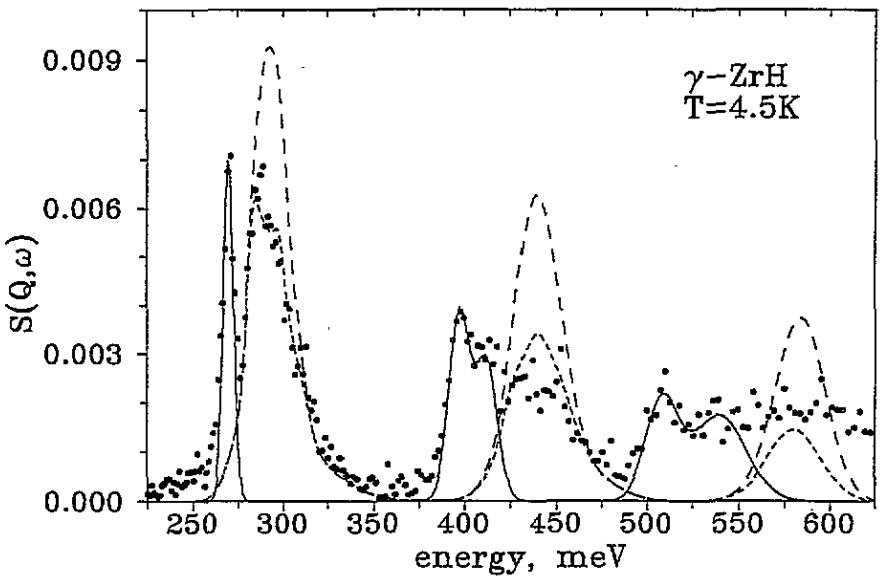

Figure 6. The high-energy range of the INS spectrum of γ-ZrH. Experimental data are shown as points. The long-dash broken curve represents the multiphonon contribution calculated in the harmonic approximation using the experimental one-phonon spectrum in the range 2–160 meV. The short-dash broken curve represents the multiphonon contribution calculated from the one-phonon spectrum with the subtracted 'anharmonic part' (see text). The full curve shows the fit with Gaussians describing the bound multiphonon bands.

The energies of bound multiphonons in γ-ZrH were determined from the positions of extra peaks in the spectrum (figure 6). Several combinations of phonon states can originate at three- and four-phonon neutron scattering when phonon binding is taken into account. Therefore, the anharmonic bands of three- and four-phonon scattering were represented as sums of two Gaussian peaks. The energies and the full widths at half maximum (FWHM, in brackets) of the attributed extra peaks are $E_2 = 269.7$ (6.7), a biphonon; $E_3 = 397$ (13.3), a triphonon, and $E_2 + \omega = 412$ (14.2), a combination of a biphonon and a phonon; $E_4 = 508$ (21), a tetraphonon, and ($E_3 + \omega$ and $2 \times E_2$) $= 539$ (35), a triphonon plus phonon and two biphonon excitations (all values are in meV). It is worth emphasizing that the bound tetraphonon is observed as a rather distinct peak in the spectrum. But we did

not attempt to give an accurate description of all four-phonon features. For example, a biphonon plus two phonons combination should noticeably contribute to the spectrum at $E_2 + 2\omega \simeq 553$ meV. Data treatment at these energies, however, was troubled due to low statistics of the spectrum, overlapping of the peaks, low spectrometer resolution at energies above 500 meV and the necessity to take into account five-phonon (four optic plus acoustic) contributions.

However, it can be seen from the calculated multiphonon spectrum in figure 1 that this spectrum gives a very good description of the left and right sides of the free two-phonon band as well as of the right side of the three-phonon band. However, there is a poor correspondence between the experimental and calculated intensities in the middle parts of these bands. Rather symmetrical negative peaks occur in the difference curve in these intervals (figure 1). The energies of the minima of the negative peaks are close to multiples of the centre of the second Gaussian, ω_2, in figure 2. We suppose therefore that the bound multiphonon states are due to binding of the 'anharmonic modes' whose energies are about ω_2.

To test this assumption we attempted to describe the harmonic multiphonon bands using a modified one-phonon band. A Gaussian peak was subtracted from the one-phonon spectrum, which was centred at an energy ω close to ω_2. The residual spectrum was used to repeat calculations of the multiphonon spectrum in the harmonic approximation. The best agreement was obtained when the subtracted Gaussian peak was centred at $\tilde{\omega} = 149$ meV and had FWHM = 10 meV, its intensity being 21% of the total intensity of the fundamental band (lower full curve in figure 2). The free two-phonon band thus calculated (short-dash broken curve in figure 6) described the experimental points with good accuracy. There is also fairly good agreement for the free three- and four-phonon bands.

The energy value, $\tilde{\omega} = 149$ meV, was used to obtain the γ-ZrH anharmonicity parameters: $A = 14$ meV and $\tilde{A} = -5.7$ meV. The width of the biphonon peak, 6.7 meV, is much lower than the convoluted width of a double-excited 'anharmonic one-phonon peak', 20 meV. This is indicative of a very resonant character of the bound multiphonons.

The outlined procedure of the data treatment was also applied to revise the analysis of INS data measured on γ-ZrD [1]. The 'anharmonic' Gaussian in the γ-ZrD spectrum had a relative intensity of 13% and $\tilde{\omega} = 107$ meV, FWHM = 4 meV. The γ-ZrD anharmonicity parameters, $A = 6.5$ meV and $\tilde{A} = -2.8$ meV, were about half those of γ-ZrH.

The anharmonicity parameters in question are of the same nature as the energy shift in higher harmonics of an anharmonic oscillator. The latter is known to have the $1/m$ dependence. Here m is the mass of the oscillator. The observed isotope dependence of the parameters A and $\tilde{A}$ for γ-ZrH(D) also follows the $1/m$ behaviour.

4. Conclusions and summary

The lattice dynamics of γ-ZrH was studied by INS. The fundamental optical hydrogen peak was observed at an energy higher than in other phases of the Zr–H system. The peak had three maxima at 141.6, 148.8 and 156.0 meV. The phonon spectrum of γ-ZrH was calculated within the Born–von Kármán model, and a good description of the experimental hydrogen optical peak was obtained. It was found that the H–H interaction in γ-ZrH is essentially the same as the D–D interaction in γ-ZrD.

In the high-energy range of the spectrum, peaks were observed below the free multiphonon bands. They were attributed to the bound multiphonon states (biphonons, triphonons, tetraphonons and their combinations) appearing in anharmonic systems.

The multiphonon contributions calculated in the harmonic approximation were compared to the experimental data. It could be estimated thereby which part of the one-phonon spectrum is responsible for the bound multiphonon states. Thus unique values of the biphonon and triphonon binding energies were obtained.

Acknowledgments

We are pleased to thank the SERC for access to the ISIS pulsed neutron source. We thank Professor V G Glebovsky of the ISSP Russian Academy of Sciences, who supplied high-purity zirconium, and Dr G Eckold (Technische Hochschule, Aachen) for providing the UNISOFT program. The research described in this paper was made possible in part by a grant from the International Science Foundation No REP000. One of us (AIK) thanks the Alexander von Humboldt Foundation for the research grant.

References

[1] Kolesnikov A I, Balagurov A M, Bashkin I O, Belushkin A V, Ponyatovsky E G and Prager M 1994 to be published
[2] Zuzek E, Abriata J P, San-Martin A and Manchester F D 1990 *Bull. Alloy Phase Diagrams* **11** 385–95, 2078–80
[3] Balagurov A M, Bashkin I O, Kolesnikov A I, Malyshev V Yu, Mironova G M, Ponyatovskii E G and Fedotov V K 1991 *Sov. Phys.–Solid State* **33** 711–4
[4] Kolesnikov A I, Balagurov A M, Bashkin I O, Fedotov V K, Malyshev V Yu, Mironova G M and Ponyatovsky E G 1993 *J. Phys.: Condens. Matter* **5** 5045–58
[5] Numakura H, Koiwa M, Asano H and Izumi F 1988 *Acta Metall.* **36** 2267–73
[6] Kolesnikov A I, Prager M, Tomkinson J, Bashkin I O, Malyshev V Yu and Ponyatovskii E G 1991 *J. Phys.: Condens. Matter* **3** 5927–36
[7] Kolesnikov A I, Bashkin I O, Malyshev V Yu, Ponyatovsky E G, Prager M and Tomkinson J 1992 *Physica* B **180 & 181** 284–86
[8] Bashkin I O, Kolesnikov A I, Malyshev V Yu, Ponyatovsky E G, Prager M and Tomkinson J 1993 *Z. Phys. Chem.* **179** 335–42
[9] Agranovich V M and Lalov I I 1985 *Sov. Phys.–Usp.* **28** 484–505
[10] Penfold J and Tomkinson J 1986 *Rutherford Appleton Laboratory Internal Report* RAL-86-019
[11] Kolesnikov A I, Natkaniec I, Antonov V E, Belash I T, Fedotov V K, Krawczyk J, Mayer J and Ponyatovsky E G 1991 *Physica* B **174** 257–61
[12] Khoda-Bakhsh R and Ross D K 1982 *J. Phys. F: Met. Phys.* **12** 15–24
[13] Hempelmann R, Richter D and Stritzker B 1982 *J. Phys. F: Met. Phys.* **12** 79–86
[14] Pelah I, Eisenhauter C M, Hughes D J and Palevsky H 1957 *Phys. Rev.* **108** 1091–2
[15] Andresen A, McReynolds A W, Nelkin M, Rosenbluth M and Whittemore W 1957 *Phys. Rev.* **108** 1092–3
[16] Woods A D 1961 *Inelastic Scattering of Neutrons in Solids and Liquids* (Vienna: IAEA) p 487
[17] Whittemore W L 1965 *Inelastic Scattering of Neutrons* (Vienna: IAEA) **2** p 305
[18] Pan S S and Webb F J 1965 *Nucl. Sci. Eng.* **23** 194–7
[19] Couch J G, Harling O K and Clune L C 1971 *Phys. Rev.* B **4** 2675–81
[20] Ikeda S and Watanabe N 1983 *Physica* B **120** 131–5
[21] Tomkinson J, Penfold J and Robertson S T 1989 *Rutherford Appleton Laboratory Internal Report* RAL-89-074
[22] Ross D K, Martin P F, Oates W A and Khoda Bakhsh R 1979 *Z. Phys. Chem.* **114** 221–30
[23] Sugimoto H and Fukai Y 1982 *J. Phys. Soc. Japan* **51** 2554–61
[24] Fukai Y and Sugimoto H 1981 *J. Phys. F: Met. Phys.* **11** L137–9
[25] Rush J J, Udovic T J, Hempelmann R, Richter D and Driesen G 1989 *J. Phys.: Condens. Matter* **1** 1061–70
[26] Hempelmann R, Richter D, Hartmann O, Karlsson E and Wäppling R 1989 *J. Chem. Phys.* **90** 1935–49

[27] Eckold G, Stein-Arsic M and Weber H-J 1986 *UNISOFT—A Program Package for Lattice-Dynamical Calculations: User Manual* (Jülich: IFF KFA) Jül-Spez-366
[28] Stassis C, Zarestky J, Arch D, McMasters O D and Harmon B N 1978 *Phys. Rev.* B **18** 2632–42
[29] Agranovich V M, Dubovskii O A and Orlov A V 1986 *Phys. Lett.* **119**A 83–8
[30] Agranovich V M and Dubovskii O A 1986 *Int. Rev. Phys. Chem.* **5** 93–101
[31] Agranovich V M, Dubovskii O A and Orlov A V 1989 *Solid State Commun.* **70** 675–81